Journal of Power Sources 273 (2015) 724–734

Contents lists available at ScienceDirect

Journal of Power Sources

journal homepage: www.elsevier.com/locate/jpowsour

Methanol oxidation on Pd/Pt(poly) in alkaline solution

A. Maksic [a], Z. Rakocevic [a], M. Smiljanic [a], M. Nenadovic [a], S. Strbac [b, *]

[a] INS Vinca, Laboratory of Atomic Physics, University of Belgrade, Mike Alasa 12–14, 11001 Belgrade, Serbia
[b] ICTM Institute of Electrochemistry, University of Belgrade, Njegoseva 12, 11001 Belgrade, Serbia

HIGHLIGHTS

- Pd nanoislands are deposited spontaneously on Pt(poly) at submonolayer coverage.
- Pd/Pt(poly) nanostructures are characterized by AFM and by spectroscopic ellipsometry.
- 35% Pd coverage exhibits superior activity for methanol oxidation in alkaline media.
- Both synergistic and electronic effects are responsible for such enhanced catalysis.
- Methanol oxidation reaction proceeds through both carbonate and formate pathways.

GRAPHICAL ABSTRACT

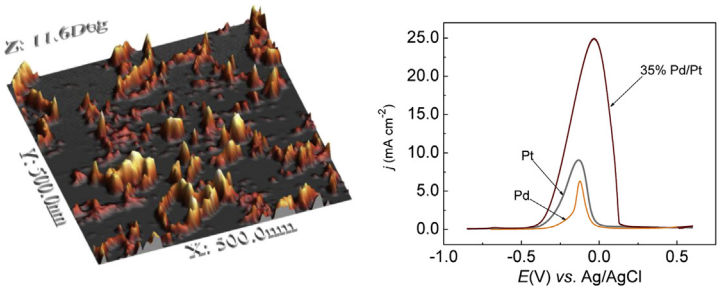

ARTICLE INFO

Article history:
Received 3 July 2014
Received in revised form
8 September 2014
Accepted 21 September 2014
Available online 28 September 2014

Keywords:
Platinum
Palladium
AFM
CO oxidation
Formaldehyde oxidation
Methanol oxidation

ABSTRACT

Bimetallic electrodes prepared by Pd nanoislands spontaneously deposited on polycrystalline platinum, Pt(poly), at submonolayer coverage were explored for methanol oxidation in alkaline media. Characterization of obtained Pd/Pt(poly) nanostructures was performed *ex situ* by AFM imaging, spectroscopic ellipsometry and by X-ray photoelectron spectroscopy. *In situ* characterization of the obtained electrodes and subsequent methanol oxidation measurements were performed by cyclic voltammetry in 0.1 M KOH. Platinum surface with 35% Pd coverage exhibited the highest catalytic activity for methanol oxidation in alkaline media, exceeding those of bare Pt and Pd. Both synergistic and electronic effects are responsible for such enhanced catalysis. The origin of the synergistic effect and possible reaction pathways for methanol oxidation were discussed taking into account the activity of obtained bimetallic electrodes for the oxidation of CO and formaldehyde, as the most probable reaction intermediates.

1. Introduction

Methanol is an energy source with a promising future as the raw material basis is broad and a growing amount of methanol is produced from renewable resources. The use of methanol as a fuel in Direct Methanol Fuel Cells (DMFCs) in which methanol is directly oxidized to CO_2 and H_2O at the anode has increased considerably in recent years. Due to very low chemical to electrical energy conversion efficiencies of DMFCs, the research is focused on the improvement of their performance through the improvement of the catalytic properties of platinum anode catalyst for methanol oxidation reaction (MOR) by the addition of another metal [1].

Scientific studies of methanol oxidation reaction on both bare platinum and platinum based electrodes have been mainly carried out in acidic electrolytes [1–4]. Methanol electro-oxidation in alkaline media has attracted increasing interest once the problems

* Corresponding author. Tel./fax: +381 11 3370 389.
E-mail address: sstrbac@tmf.bg.ac.rs (S. Strbac).

http://dx.doi.org/10.1016/j.jpowsour.2014.09.138
0378-7753/

related to the use of methanol in fuel cells, such as carbonation and deactivation of the alkaline electrolyte due to CO_2 retention and unavailability of appropriate alkaline anion exchange membranes, were resolved [5]. It was found that the use of alkaline electrolytes offered several advantages including much wider range of electrode materials that are stable in an alkaline media and their higher electrocatalytic activity for the oxidation of organic fuels in comparison with their activity in acidic media [6–8].

Methanol oxidation reaction on platinum electrodes in alkaline media proceeds either through carbonate or through formate pathways involving different adsorbed intermediates and byproducts during the oxidation process [6–10]. The overall methanol oxidation reaction leading to carbonate as a product:

$$CH_3OH + 8OH^- \rightarrow CO_3^{2-} + 6H_2O + 6e^- \quad (1)$$

proceeds through several elementary steps involving CO as an adsorbed poisoning intermediate [6,7]. The other pathway with the formate as a product, and the overall reaction:

$$CH_3OH + 5OH^- \rightarrow HCOO^- + 4H_2O + 4e^- \quad (2)$$

includes also several elementary steps with formaldehyde and the other different reaction intermediates [8,9].

Many authors have already shown that the methanol oxidation reaction can proceed through parallel reaction pathways [7,8,11]. In some cases large amounts of liquid products such as formaldehyde and formate are produced together with the formation of both linear and bridge bonded CO, which are formed in carbonate pathway and act as poisoning species [7–10]. However, although electrocatalytic activity for the MOR in alkaline solutions is generally high, the presence of liquid products such as formaldehyde and formate indicate an incomplete oxidation of methanol due to the poisoning of the electrode surface by strongly adsorbed CO [10]. Therefore, the main challenge in methanol electrocatalysis on platinum based electrodes is to find a catalyst that can favor adsorption and complete oxidation of formyl species and to avoid the subsequent formation of adsorbed CO by blocking neighboring platinum sites or to oxidize it at lower potentials.

The most promising way to increase the electrocatalytic activity of platinum based electrodes towards methanol oxidation is to modify platinum with a second metal, like Ru, Sn, Mo, Bi [2,12]. The enhanced catalytic activity of such bimetallic surfaces is achieved either through bifunctional or through electronic effect or a combination of both [11,12]. Different methods of modifying platinum electrode with a second metal were employed, for instance PtRu, the most efficient catalyst for methanol oxidation in both acid and alkaline solutions, could be prepared either by Ru electrodeposition [13], UHV evaporation [14], spontaneous deposition [15] on various Pt substrates, or various PtRu nanoparticles could be carbon supported [16,17].

Although Pd has shown lower activity for methanol oxidation in alkaline solution than Pt [18], a combination of two metals prepared either by evaporation and electrochemical deposition of Pd on Pt substrates [19] or by carbon supported PtPd nanoparticles [20], has shown better catalytic activity than bare Pt. Spontaneous deposition method is chosen in this work because of its simplicity and the fast surface coverage plateau reached as revealed through open circuit potential changes during Pd deposition on Pt(poly) [21]. Different Pd/Pt(poly) nanostructures were prepared with respect to Pd nanoislands coverage only by using different deposition times for a given Pd containing solution.

The scope of this paper is to examine the electrocatalytic activity of obtained Pd/Pt(poly) nanostructures for methanol oxidation in alkaline solution. Ex situ characterization of different Pd/Pt(poly) nanostructures was performed by atomic force microscopy (AFM), spectroscopic ellipsometry and by X-ray photoelectron spectroscopy (XPS), while methanol electro-oxidation studies were performed using electroanalytical techniques. An enhanced activity of Pd/Pt(poly) nanostructures for methanol oxidation in alkaline solution with respect to both bare Pt and Pd was correlated with Pd surface coverage. Additionally, the activity of Pd/Pt(poly) bimetallic electrodes towards the oxidation of CO and formaldehyde as the most possible intermediates during methanol oxidation was investigated in order to get a better insight into the possible reaction pathways.

2. Experimental

2.1. Chemicals

Suprapure sulfuric acid (Merck) and $PdCl_2$ (Alfa Aesar) were used for the depositing solutions. Working solutions were prepared with potassium hydroxide pellets provided by Merck and Millipure water. Solutions were deoxygenated by a flow of 99.999% N_2 supplied by Messer. Methanol (Merck), formaldehyde (Merck) and high purity CO (Messer) were used for electrocatalytic measurements.

2.2. Preparation of Pd/Pt(poly) bimetallic electrodes

Pt(poly) disc electrode, 5 mm in diameter (Pine Instruments Co.), was modified by a spontaneous deposition of Pd during immersion of platinum electrode at an open circuit potential (OCP) into (1 mM $PdCl_2$ + 0.05 M H_2SO_4) solution for 1, 3 and 30 min (further in the text referred to as the deposition time). Before each experiment, the electrode was cleaned by electrochemical polishing through surface oxidation/reduction in perchloric acid solution. The same procedure was applied for the removal of Pd deposit after each experiment.

2.3. Height and phase AFM imaging

Obtained Pd/Pt(poly) nanostructures were characterized *ex situ* by tapping mode AFM using Multimode Quadrex SPM with NanoScope IIIe controller (Veeco Instruments, Inc.), and a commercial Veeco RFESP AFM probe (NanoScience Instruments, Inc.). Height and phase AFM images were acquired simultaneously from various areas over the electrode surface. While height AFM images are sensitive to surface topography, corresponding phase images are sensitive mainly to surface chemical composition, which was demonstrated in detail for the same Pd/Pt(poly) system in Ref. [21]. Surface roughness and the size of the deposited Pd islands are estimated from height AFM images, while coverage taken as a percentage of Pt(poly) surface covered with Pd islands is estimated from phase AFM images. Image processing was performed by Veeco NanoScope III program and also by WSxM SPM software [22].

2.4. Spectroscopic ellipsometry measurements

Spectroscopic ellipsometry was used for the additional characterization of Pd nanoislands spontaneously deposited on Pt substrate. HORIBA Jobin Yvon UVISEL iHR320 with monochromator wavelength range from 250 to 850 nm (1.5 up to 4.8 eV) and with a step of 0.1 eV was employed for these measurements. The incident angle was set at 70° and the light spot was 1 mm in diameter. All optical spectra were recorded *ex situ* immediately after spontaneous deposition, and under the same conditions for all electrodes. Further analysis of the obtained optical spectra was performed by fitting the experimental data using the commercial software

package DeltaPsi 2, in order to estimate the average height of Pd islands on Pt(poly) substrate. Standard fit of the experimentally measured Is and Ic signal intensities was used according to the following equations:

$$Is = \sin(2\Psi)\cdot\sin(\Delta) \quad (3)$$

$$Ic = \sin(2\Psi)\cdot\cos(\Delta) \quad (4)$$

where, Ψ is the amplitude change of the reflected wave, while Δ is the phase change of the same reflected light beam. Software package DeltaPsi 2 gives an explicit form of the dependence of the refractive index, n, and of the extinction coefficient, k, on the wavelength [23].

2.5. X-ray photoelectron spectroscopy measurements

X-ray photoelectron spectroscopy analysis of as received samples was carried out using SPECS System with XP50M X-ray source for Focus 500 and PHOIBOS 100/150 analyzer. AlKα source (1486.74 eV) at a 12.5 kV and 32 mA was used for this study. XPS spectra were obtained at a pressure in the range of $3 \times 10^{-8} - 2 \times 10^{-9}$ mbar. Survey spectra were recorded from 0 to 1000 eV, with the energy step of 0.1 eV, dwell time of 0.5 s, and with pass energy of 40 eV in the Fixed Analyzer Transmission (FAT) mode. Relevant regions were identified from survey spectra to be: Pt 4f (64–80 eV), Pt 4d and Pd 3d (350–300 eV) and O 1s (540–525 eV). Region spectra were recorded with the energy step of 0.1 eV, dwell time 2 s and pass energy of 20 eV in the FAT mode. Spectra were collected by SpecsLab data analysis software and analyzed by CasaXPS software package both supplied by the manufacturer.

2.6. Electrochemical measurements

Electrochemical measurements were carried out in a conventional three electrode cell, where Pd modified Pt(poly) was used as working electrode, while Pt wire and Ag/AgCl, 3 M KCl were used as counter and reference electrodes, respectively. Experimental data were acquired and processed using Pine instruments bipotentiostat AFCBP1. Electrochemical characterization of Pd modified Pt(poly) surfaces was performed by cyclic voltammetry (CV) measurements in oxygen free 0.1 M KOH. In a separate set of experiments, CO stripping voltammetry was carried by CO admitted to the solution for 10 min at the potential of −0.85 V, followed by purging CO out of the solution using high purity nitrogen for 20 min. Formaldehyde oxidation and methanol oxidation reactions on Pd/Pt(poly) surfaces were examined in the same oxygen free 0.1 M KOH solution containing either 0.4 M formaldehyde or 0.4 M methanol. Each CV experiment was preceded with holding the electrode potential at −0.85 V for 15 min in order to get more stable deposit by its reduction to the metallic state. For comparison all electrochemical measurements were also carried out on bare Pt(poly) and bare Pd(poly) disc (5 mm in diameter, Pine Instruments Co.) electrodes.

3. Results and discussion

3.1. Characterization of Pd/Pd(poly) bimetallic electrodes

3.1.1. Ex situ characterization of Pd/Pt(poly) surfaces by height and phase AFM imaging

AFM images of a bare Pt(poly) surface were shown and discussed in detail in our previous paper [21]. Briefly, height images showed that surface topography of Pt(poly) consisted of various facets giving the average surface roughness of 2.0, while phase image indicated the presence of 1.5% of impurities on the surface.

Height and phase AFM images of Pd/Pt(poly) nanostructures obtained for the deposition times of 1, 3 and 30 min are presented in Fig. 1. From height AFM image showing the topography of Pd/Pt(poly) nanostructure obtained after 1 min Pd deposition, Fig. 1a, the average surface roughness is estimated to be 2.03, while from cross section analysis, as illustrated in Fig 1b, the island heights ranged from 0.25 to 1.0 nm and the island sizes ranged from 5 to 30 nm. From a corresponding phase AFM image, Fig. 1c, the estimated coverage is 25 ± 5%. From height AFM image of Pd/Pt(poly) nanostructure obtained after 3 min Pd deposition, Fig. 1d, the average surface roughness is estimated to be 2.08, while from cross section analysis, Fig 1e, the island heights ranged from 0.5 to 2 nm and the island sizes ranged from 10 to 30 nm. From phase AFM image, Fig. 1f, the estimated coverage is 38 ± 5%. Surface topography AFM image for Pd/Pt(poly) surfaces obtained after 30 min Pd deposition, Fig. 1g, gives the average surface roughness of 2.1. Cross section analysis, Fig. 1h, gives that Pd islands heights ranged from 2 to 4 nm, while the island sizes ranged from 10 to 60 nm. From a corresponding phase AFM image, Fig. 1i, the calculated coverage of 52 ± 5% is in accordance with our previously published results [21]. It is interesting to note that although the growth of randomly distributed Pd islands occur in all cases, with increasing the deposition time, the island heights increase much more than the island widths. This indicates that at particular domains of polycrystalline Pt surface, layer growth prevails in the beginning, followed by the island growth on top, according to the well-known Stranski–Krastanov growth mode.

3.1.2. Ex situ characterization of Pd/Pt(poly) surfaces by spectroscopic ellipsometry

Pd/Pt(poly) bimetallic electrodes were subjected to spectroscopic ellipsometry measurements in order to get a better insight into the structure of the deposit. The nanoscale height of Pd islands makes them convenient for ellipsometric characterization, because of its partial transparency in the used wavelength range. The optical spectra of modified electrodes were recorded *ex situ* and as an illustration, the obtained results of one of them (35% Pd/Pt(poly)), along with the spectra of bare Pt and Pd are given in Fig. 2. The refractive index, n, and the extinction coefficient, k, parameters are given as a function of the wavelength at separate graphs in Fig. 2a and b, respectively. The optical spectra of Pd modified Pt(poly) surface differ from both bare Pt and Pd. Compared to bare Pt, the changes of the refractive index, Fig. 2a, which describe how light travels through the sample, are more pronounced than the changes of the extinction coefficient, Fig. 2b, which refer to the light absorption. Both spectra are closer to the ones for bare Pt substrate than for bare Pd, which is reasonable since the amount of the deposited Pd on 35% Pd/Pt(poly) is much smaller than the amount of Pt. As revealed from AFM images, deposited Pd islands are randomly distributed over Pt substrate surface, and not homogenous in size, which leads to the more pronounced changes of the refractive index. On the other hand, only a slight change of the extinction coefficient values could be explained by the similar metallic nature of all examined samples.

The average heights of Pd nanoislands are extracted from the optical spectra by fitting the experimentally recorded curves. Apart from the data experimentally obtained by ellipsometry as described above, the input parameter for the simulation of the Pd islands height was the coverage of Pt with the deposited Pd islands. According to the data estimated from phase AFM images (see above), coverage values of 25%, 35% and 50% were taken for Pd/Pt(poly) bimetallic electrodes obtained for 1, 3 and 30 min Pd deposition time, respectively. For 25% Pd/Pt(poly) and 35% Pd/Pt(poly), the obtained simulated average heights of Pd islands were 0.5 ± 0.1 nm and 2.9 ± 0.3 nm, respectively, with the standard

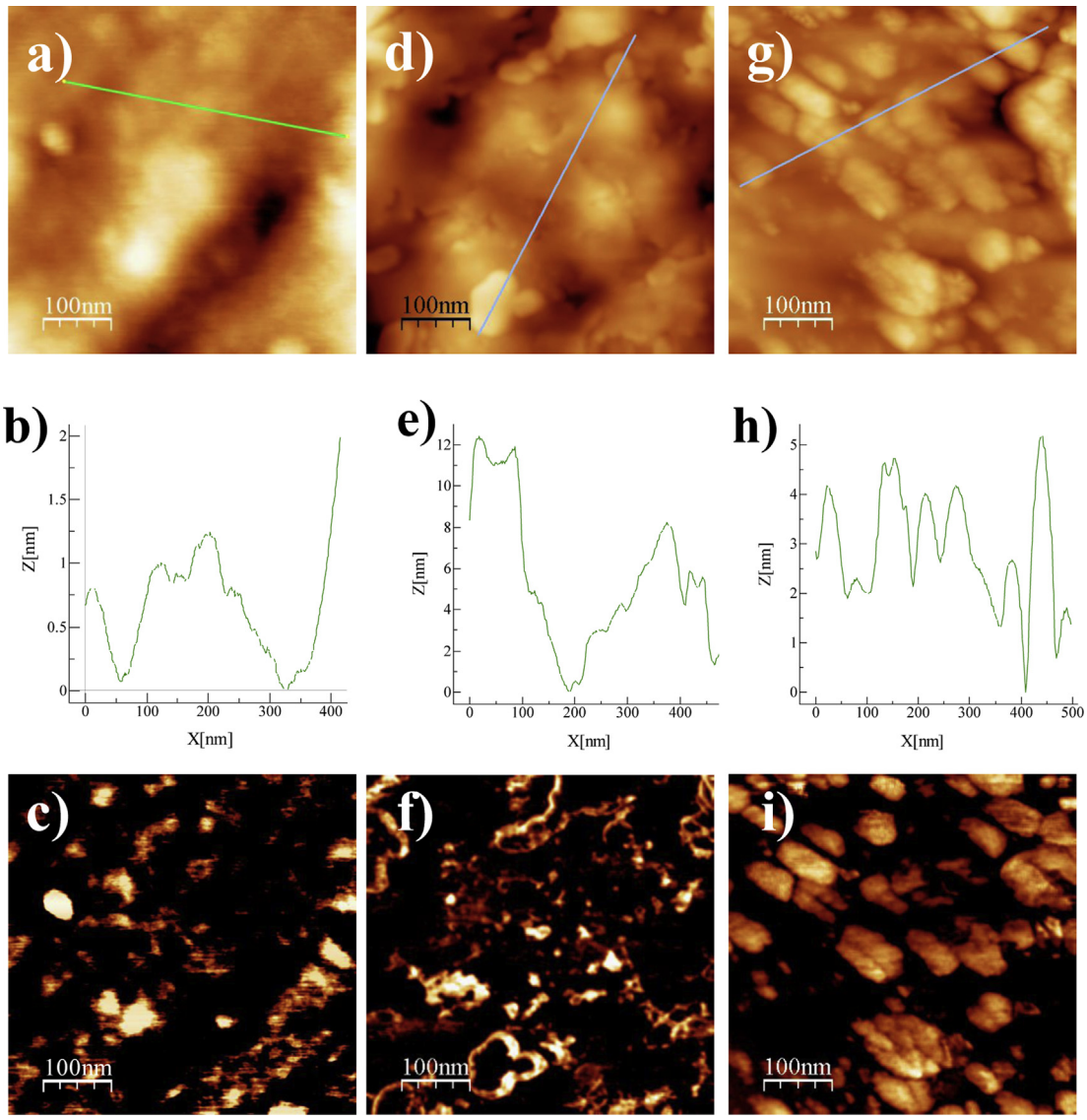

Fig. 1. AFM images (500 × 500) nm^2 of Pd/Pt(poly) surfaces obtained after 1 min (left column), 3 min (middle column) and 30 min (right column) Pd deposition showing: a) surface topography, *z*-range 4.6 nm; b) cross section along the line indicated in the image; and c) composition in corresponding phase image, *z*-range 1.3°; d) surface topography, *z*-range 38.9 nm; e) cross section along the line indicated in the image; and f) composition in corresponding phase image, *z*-range 20.3°; g) surface topography, *z*-range 12.0 nm; h) cross section along the line indicated in the image; and i) composition in corresponding phase image, *z*-range 14.2°.

deviation value during simulation of 0.5. For 50% Pd/Pt(poly), simulated Pd islands average height was 4.8 ± 0.4 nm, with the standard deviation value during simulation of 0.6.

Heights of Pd nanoislands deposited on Pt substrate extracted from ellipsometric simulation and from AFM images are somewhat different. This could originate from the fact that AFM analysis gives an excellent insight into the surface properties at the nanoscale, while ellipsometry gives an overall view into bimetallic surface properties. Besides, due to the nonuniformity of the deposited Pd islands with respect to the island heights at submonolayer coverage, it is more likely that the real average values are observed by ellipsometry than by AFM. The average Pd island height varies for different AFM images obtained over a number of different surface areas and ranged from 0.25 to 1.0 nm for 1 min deposition, 2–4 nm for 3 min deposition to 4–7 nm for 30 min deposition [21]. We demonstrate here that for good statistics, instead of recording a number of AFM images, better and much faster estimation of the average island heights over a wider surface area can be obtained from ellipsometry measurements.

The content of Pd on Pd/Pt(poly) can be calculated from the average height of Pd islands taken from ellipsometry (0.5 nm, 2.9 nm and 4.8 nm for 1, 3 and 30 min deposition time, respectively), multiplied by: the geometric area of the electrode (0.196 cm^2), Pd deposit coverage, and by palladium density (12.023 g cm^{-3}). For 25%, 35% and 50% Pd/Pt(poly), Pd content is calculated to be 0.03 μg, 0.24 μg and 0.57 μg, respectively. It is worth noting that in this case, where Pt(poly) as substrate is very active for methanol oxidation, Pd content is very low, approximately 100–1000 times lower than the loading needed for Pd/C systems [24–26], where carbon substrate is not active for methanol oxidation.

3.1.3. XPS analysis of Pd/Pt(poly) nanostructures

High resolution XPS spectra for Pt 4f, Pt 4d, Pd 3d, and O 1s regions recorded from as received 50% Pd/Pt(poly) substrate, are presented in Fig. 3. In Fig. 3a, Pt 4f photoelectron line, corresponding to platinum substrate is presented. This line was fitted to two contributions corresponding to Pt(0) (89%, positioned at

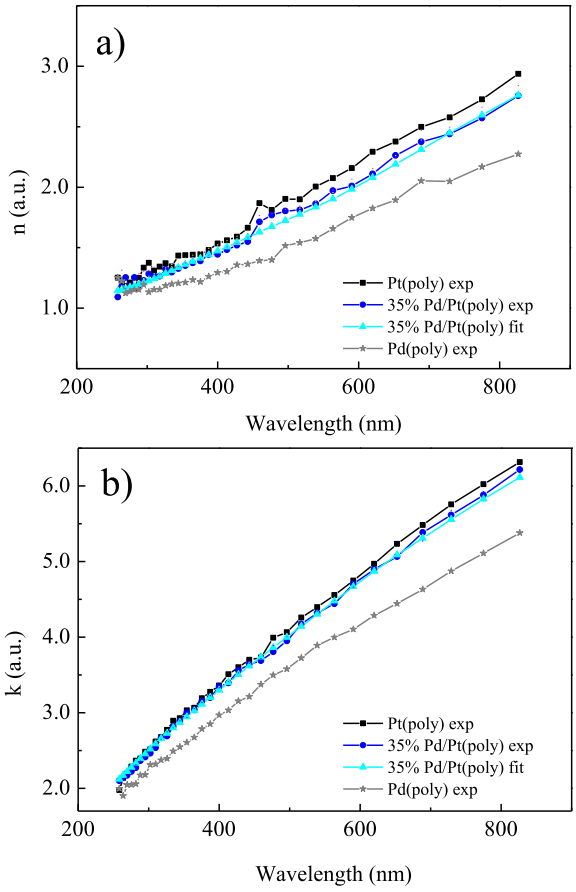

Fig. 2. Ellipsometric spectra of bare Pt(poly), Pd(poly) and 35% Pd/Pt(poly) nanostructure, showing the experimentally obtained and fitted values of: a) the refractive index; b) the extinction coefficient.

71.2 eV, blue line (in web version)) and to Pt^{2+} (11% positioned at 72.2 eV, red line), attributed to metallic Pt and PtO, respectively [27]. The origin of PtO phase is most likely related to the oxidation due to the air exposure. This is further supported by the analysis of O 1s line, shown in Fig. 3b). This line was fitted to two contributions: the dominant one at 532,8 eV, is related to C–O bonds originating from contamination due to the air exposure, while the second one at 531,2 eV is closest to PtO contribution [28]. It is worth noting that the later contribution of O 1s cannot be attributed to either oxygen adsorbed on Pd (529.0 eV), or PdO (529.6 eV) [29]. However, the presence of Pd–O bonds cannot be excluded knowing that the relative amount of Pd is much smaller than that of Pt.

The presence of Pd and its oxidation state is revealed from the detailed analyses of Pd 3d line, shown in Fig. 3c. Since this line is overlapped with much more intensive Pt 4d line, they were resolved by the fitting to four different contributions (two for each line). Peaks related to Pd 3d lines are very narrow, implying the presence of a single chemical state. The position of Pd $3d_{5/2}$ at 335.8 eV fits perfectly to metallic Pd on which oxygen is adsorbed [30].

3.1.4. Cyclic voltammetry characterization of Pd/Pt(poly) surfaces in 0.1 M KOH

Cyclic voltammograms of Pd/Pt(poly) surfaces obtained after 1, 3 and 30 min Pd deposition, as well as CV of a bare Pt(poly) surface recorded in 0.1 M KOH solution in the same potential limits from −0.85 to 0.60 V are shown in Fig. 4. CV of a bare Pt exhibits all

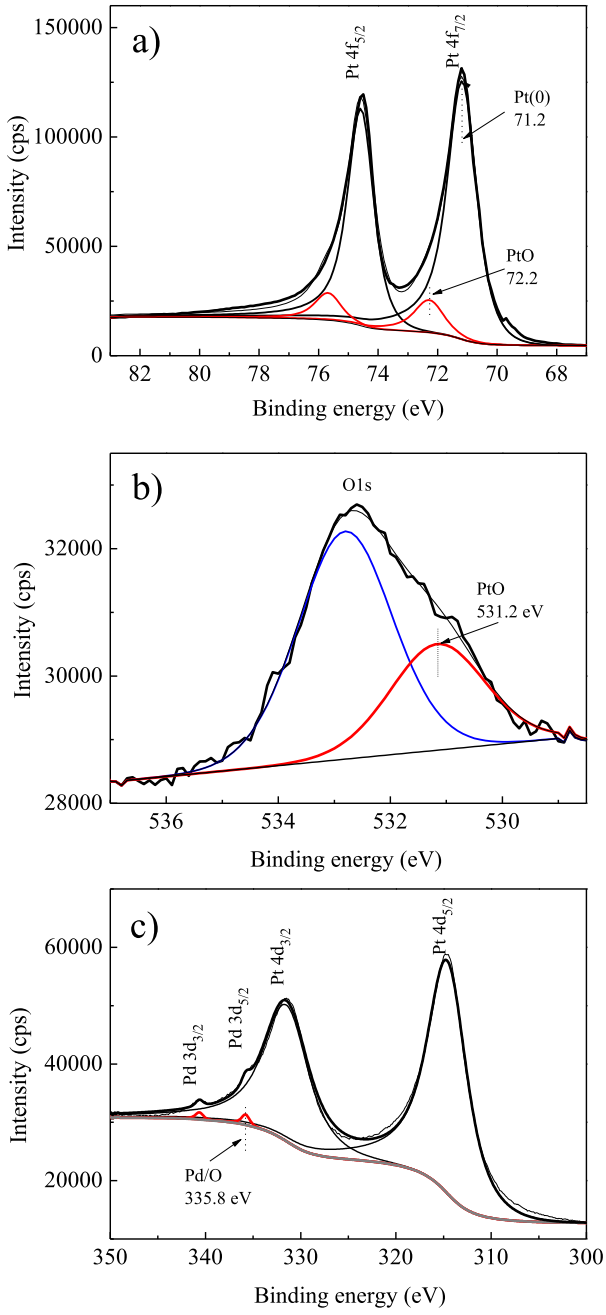

Fig. 3. High resolution XPS spectra of: a) Pt 4f; b) O 1s; c) Pd 3d and Pt 4d. The spectra were taken from as received Pd/Pt(poly) sample, obtained by spontaneous deposition of palladium on Pt(poly) from (1 mM $PdCl_2$ + 0.05 M H_2SO_4) for 30 min, and after rinsing with water. Positions of different phases are denoted by arrows.

known features in alkaline solution [31,32]. Hydrogen adsorption/desorption peaks, which on bare Pt(poly) appear at −0.68 V are suppressed due to the presence of Pd islands, while the peak which appear at −0.56 V is also suppressed for Pd/Pt(poly) surface obtained after 3 min Pd deposition, and almost disappear for Pd/Pt(poly) obtained after 30 min Pd deposition. According to ref [33], the peak at lower potentials for hydrogen adsorption on Pd monolayer deposited on Pt(111) in perchloric acid solution is shifted towards more positive potentials with respect to bare Pt because Pd–H interaction is stronger than Pt–H interaction. On the other hand, at higher potentials Pd monolayer is oxidized due to the oxophilic nature of Pd deposit, which led to the suppression of $H_{ads/}$

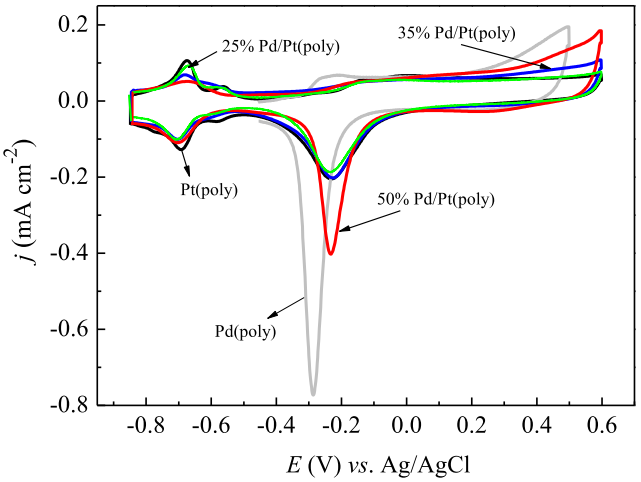

Fig. 4. CV profiles of bare Pt(poly) and of Pt(poly) surfaces modified with spontaneously deposited Pd, recorded in 0.1 M KOH in the potential region from −0.85 V to 0.6 V, and at a scan rate of 50 mV s^{-1}. CV profile of bare Pd(poly) surface is recorded in the same solution in the potential range from −0.5 V to 0.5 V.

$_{des}$ peaks. In our case, the shift of $H_{ads/des}$ peaks at −0.68 V to the more positive potential is due to the higher Pd−H interaction, while the suppression of $H_{ads/des}$ peaks at the potential of −0.56 V is due to the at least partial oxidation of the deposited Pd islands, which is even more pronounced in alkaline solution due to the high concentration of OH^- anions. The suppression of $H_{ads/des}$ on Pd/Pt(poly) increases with the increase of Pd coverage. Taking into account that hydrogen does not adsorb on one or two monolayer high Pd deposit on Pt [33], Pd coverage is estimated from the suppression of H_{ads} peaks similarly like in Refs. [21], which gives approximately: (15 ± 5)%, (32 ± 5)%, and (45 ± 5)%, for 1, 3 and 30 min Pd deposition, respectively. These values are slightly lower than ones estimated from AFM images, and do not take into account the adsorption of hydrogen on non-oxidized Pd islands. Besides, the change in the electrochemically active surface area (see below) after Pd deposition also contributes to the accuracy of Pd coverage estimation from H_{ads} peaks. Therefore, the mean values for Pd coverage taken from AFM images: 25%, 35% and 50%, for 1, 3 and 30 min Pd deposition, respectively, will be used further in this work.

Enlarged double layer in the potential region from −0.5 V to −0.2 V, which is for bare Pt(poly) ascribed to the reversible adsorption of OH^- anions and PtO formation/reduction [31,32,34,35] is also modified by the presence of Pd nanoislands. For Pd coverage of 25% and 35%, both OH^- adsorption and PtO formation begin at more negative potentials compared to bare Pt(poly), while in the reverse scan, the oxide reduction peaks almost coincide with the one for Pt(poly) at −0.23 V, indicating a strong influence of Pt substrate for lower Pd coverage, and a simultaneous reduction of both Pt and Pd oxides. On the other hand, for Pd coverage of 50%, particularly sharp and large oxide reduction peak appears slightly shifted to the more negative potential, and resembling the peak for palladium oxide reduction at −0.29 V (see CV curve of bare Pd given in Fig. 4). According to literature [36–38], this peak corresponds to the reduction of Pd^{2+}. For 35% and 50% Pd/Pt(poly) surfaces, this peak is preceded with a broad shoulder in the potential region from 0.48 to 0.01 V, which is attributed to the reduction of high valence Pd oxides (Pd^{4+}) [36–38]. Moreover, the formation of high valence non-reducible palladium oxides can also be assumed. (In order to avoid the formation of high valence palladium oxides, the upper potential limit for bare Pd(poly) shown in Fig. 4, was set at lower value of 0.5 V).

3.2. Activity of Pd/Pt(poly) surfaces for the oxidation of possible reaction intermediates

Methanol oxidation reaction proceeds either through carbonate or through formate pathways involving adsorbed CO and formaldehyde, respectively, as the main intermediates (see Introduction). Therefore, it was challenging to investigate the activity of obtained Pd/Pt(poly) electrodes towards these possible intermediates in order to get a better insight into their activity and possible reaction pathways during methanol oxidation in the same alkaline media.

3.2.1. CO stripping voltammetry on Pd/Pt(poly) surfaces in 0.1 M KOH

CO stripping voltammetry results for different Pd/Pt(poly) nanostructures, as well as for bare Pt(poly) and Pd(poly) are presented in Fig. 5, together with CVs recorded in the same, but CO free 0.1 M KOH solution presented by dotted lines. Pt(poly) exhibits the highest activity for CO electrooxidation in alkaline media since the onset potential of −0.75 V is the most negative and falls in hydrogen desorption potential region, as can be seen in Fig. 5a. This high activity of polycrystalline platinum electrode for CO oxidation has already been reported by numerous authors [39–41]. The main peak for CO oxidation is centered at −0.26 V, while two prepeaks are centered at −0.54 V and −0.33 V. These different peaks can be explained by different CO adsorption energies on various Pt sites. Namely, after a certain amount of CO molecules adsorbed at the platinum surface were oxidized in the prepeak potential region, all lateral repulsions among remaining CO molecules became reduced and as a consequence, the bond between CO and platinum became stronger [40,41].

Stripping voltammetry curves for CO oxidation on Pd/Pt(poly) electrodes with different palladium coverage are shown in Fig. 5b, c and d. The presence of Pd islands with the coverage of 25% and 35%, Fig. 5b and c, causes the shift of the main CO stripping to the more positive potentials for 10 mV and 30 mV, respectively, with respect to the peak potential for CO stripping on bare Pt(poly). CO stripping prepeaks are slightly suppressed and also slightly shifted to the more positive potentials. For Pd coverage of 50%, Fig. 5d, CO stripping prepeaks dissapear almost completely, while the main CO stripping peak is shifted positively for 80 mV compared to bare Pt. This positive peaks shift means that the presence of palladium on platinum surface contributes to the enhancement of the bond between CO and platinum. The increase in the binding energy may be caused by the modification of the electronic properties of platinum substrate by the deposited palladium islands [42]. This is in accordance with CO electrooxidation on bare Pd(poly) electrode, which occurs at only 45 mV more positive potential, Fig. 5e, than the same one on 50% Pd/Pt(poly). FTIR spectroscopic study revealed that CO species are bridge bonded to Pd sites ($Pd_2C{=}O$) and that a complete removal of CO species may not be possible at low potentials, as they are strongly bonded to the electrode surface [43]. This means that much more positive value of the peak potential for CO stripping on palladium than on platinum is due to the fact that CO is adsorbed more strongly on palladium than on platinum [42,44].

Electrochemically active surface area can be estimated from CO stripping charges taking into account the charge of 420 μC cm^{-2}, for a full CO monolayer adsorbed on Pt [24], (similar charge of 424 μC cm^{-2} is reported for a full CO monolayer on Pd [37]). For Pt(poly) and Pd(poly), the electrochemically active surface areas are equal to the geometric surface area of 0.198 cm^2, while for 25%, 35% and 50% Pd/Pt(poly) calculated values are: 0.220 cm^2, 0.242 cm^2 and 0.251 cm^2, respectively.

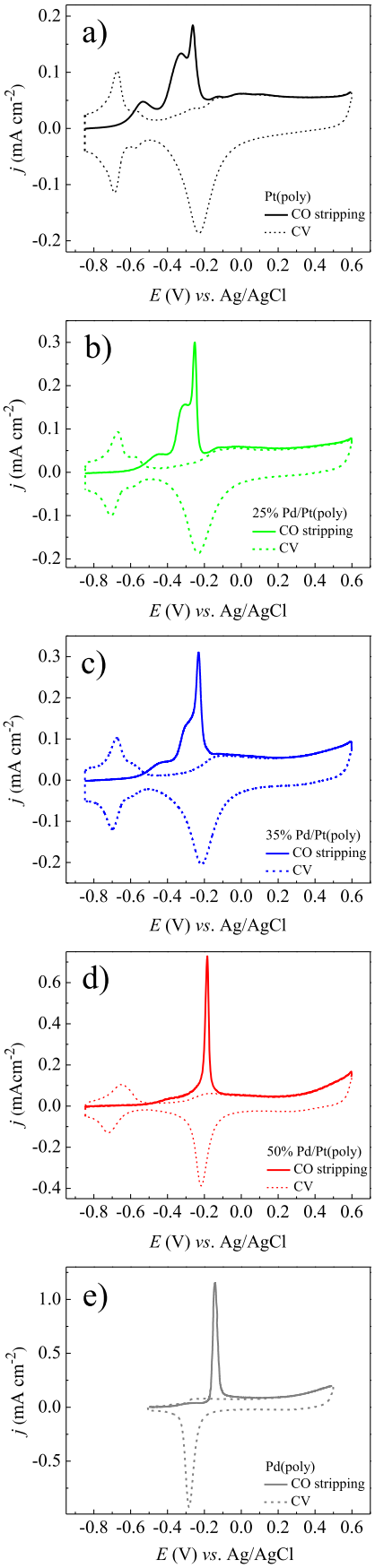

Fig. 5. CO stripping voltammetry of: a) Pt(poly); b) 25% Pd/Pt(poly); c) 35% Pd/Pt(poly); d) 50% Pd/Pt(poly), and e) Pd(poly) in 0.1 M KOH. Stripping curves were recorded at a scan rate of 50 mV s^{-1}. Corresponding CVs recorded after CO stripping, presented by dotted lines, are in a good agreement with CVs obtained before (see Fig. 4).

3.2.2. Formaldehyde oxidation on Pd/Pt(poly) in 0.1 M KOH

CVs for formaldehyde oxidation on Pt(poly), 25%, 35%, 50% Pd/Pt(poly) and bare Pd(poly) recorded in (0.4 M HCHO + 0.1 M KOH) are presented in Fig. 6. Pd(poly) exhibits the lowest activity for HCHO oxidation. Reaction begins at −0.4 V, and the maximum current density of 10 mA cm^{-2} is achieved at −0.16 V. The activity of Pt(poly) is higher with the initial potential of −0.5 V and the maximum current density of 13.4 mA cm^{-2}, which is achieved at lower potential of −0.18 V. The activity of both 25% and 35% Pd/Pt(poly) is higher than that of both consisting metals, as revealed from 30 mV shift of the initial potential to the more negative values with respect to the most active Pt, although with increasing potential, formaldehyde oxidation becomes hindered on 25% Pd/Pt(poly) surface. On the other hand, for 50% Pd/Pt(poly), HCHO oxidation begins at slightly more positive potential compared to bare Pt, but at more negative compared to bare Pd. In all cases, maximum current densities are lower than the one for bare Pt, but higher than the one for bare Pd. The enhanced activity of 25% and 35% Pd/Pt(poly) for HCHO oxidation, exceeding the activity of both consisting metals with respect to the initial potential, indicates the synergistic effect. The origin of this synergy is most likely in the oxidation state of the deposited Pd islands. According to CVs from Fig. 4, in the potential region of HCHO oxidation PdOH is present on the surface. Besides, the electronic modification of the deposited Pd islands by Pt substrate leads to the lowering of a binding energy of adsorbed reaction species and consequently to the lowering of the overpotential for HCHO oxidation.

3.3. Methanol oxidation on Pd/Pt(poly) surfaces in 0.1 M KOH

CVs for the electrochemical oxidation of methanol on three different Pd/Pt(poly) nanostructures and on bare Pt(poly) and Pd(poly) in 0.4 M CH_3OH + 0.1 M KOH are presented in Fig. 7. In the forward sweep, methanol oxidation on bare Pt(poly) surface begins at the potential of −0.45 V, which according to the CV from Fig. 4, corresponds to the beginning of PtOH formation, and proceeds with an increasing current reaching a maximum value of 9 mA cm^{-2} at −0.13 V, after which the oxidation current decreased and reached a zero value at a potential of 0.2 V, corresponding to the formation of a full PtOH monolayer. In the reverse sweep, CH_3OH oxidation proceeds over a significantly narrower potential region with a current maximum much lower than in the anodic direction indicating that the intermediate species formed in the forward sweep, remained adsorbed at or stayed in the vicinity of the electrode surface. The activity of bare Pd(poly) for methanol oxidation is much lower than that of bare Pt, and in the forward sweep occurs in the potential region from −0.32 V corresponding to the beginning of PdOH formation (see CV from Fig. 4) up to formation of a full PdOH monolayer at 0.07 V. Maximum current density of 6.3 mA cm^{-2} is achieved at −0.13 V. In the reverse sweep methanol oxidation occurs in a narrow potential region from −0.25 V to −0.35 V showing very small current density.

Methanol oxidation curves on three different Pd/Pt(poly) nanostructures have shown that the activity of the platinum surface with 35% Pd coverage is more pronounced than the one with 25% Pd coverage, and highly exceeds the one with 50% Pd coverage. Methanol oxidation on 25% and 35% Pd/Pt(poly) occur in the potential region from −0.5 up to 0.22 V. For the most active 35% Pd/

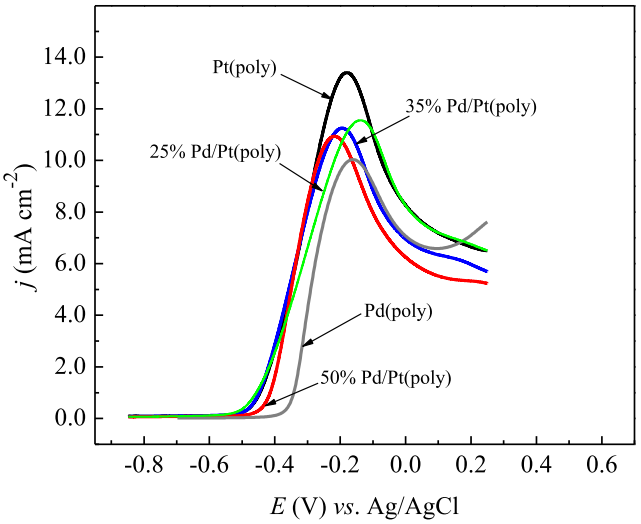

Fig. 6. Formaldehyde oxidation on Pt(poly), Pd(poly), and on 25%, 35% and 50% Pd/Pt(poly) in (0.4 M HCHO + 0.1 M KOH). First sweeps in the anodic and cathodic directions were recorded at a scan rate of 50 mV s^{-1}. Current densities are referred to the electrochemically active surface areas.

Pt(poly) surface, the maximum current density of 20.4 mA cm^{-2} is achieved at −0.04 V, exceeding thus significantly the activity of platinum, the most active pure metal. On the other hand, the activity of 50% Pd/Pt(poly) for methanol oxidation is much lower, and the reaction begins at potential more positive than on Pt and proceeds with current densities comparable to those for bare Pt. Ratio between the backward, Ib, and forward, If, peak current densities during the electrooxidation of methanol indicates the susceptibility of the electrode surface for the poisoning with the adsorbed reaction intermediates [17]. For the bare Pt substrate, Ib/If ratio was 0.22, while the same Ib/If value was calculated for Pd(poly) electrode, indicating a similar vulnerability of these two basic surfaces for poisoning with adsorbed intermediates. For 35% Pd/Pt(poly) this ratio was 0.20, indicating less poisoning, while for 25% and 50% Pd/Pt(poly) it increased to 0.22 and to 0.27, respectively, thus making them more susceptible to deactivation due to the adsorption of poisoning intermediates. From the comparison of the activities of

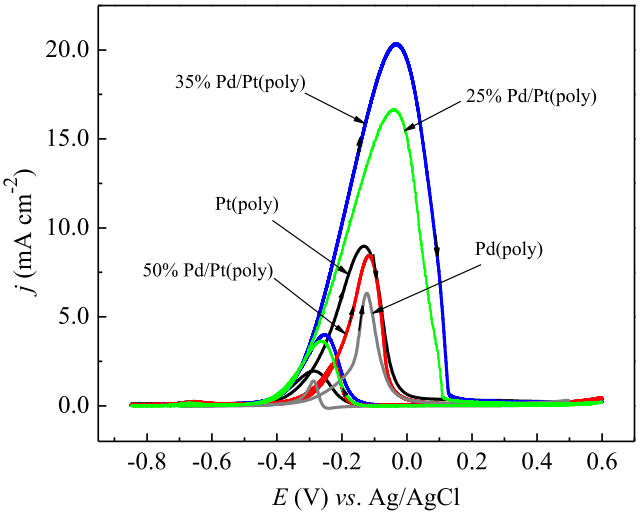

Fig. 7. Methanol oxidation on Pt(poly), Pd(poly), and on 25%, 35% and 50% Pd/Pt(poly) in (0.4 M CH_3OH + 0.1 M KOH). First sweeps in the anodic and cathodic directions were recorded at a scan rate of 50 mV s^{-1}. Current densities are referred to the electrochemically active surface areas.

Pd modified Pt(poly) electrode with the activities of bare Pt and Pd for methanol oxidation one can see that at lower potentials, the oxidation of methanol takes place mainly at the platinum sites of the modified electrode and most likely on the edges of Pd islands. This means that 35% palladium coverage is low enough to enable a high percentage of platinum utilization as well as that it provides enough Pd/Pt edges, which are active for the adsorption and oxidation of reaction intermediates, hence the noticed highest electrocatalytic activity. On the other hand, 25% Pd coverage indicates the lack of enough Pd/Pt edges, while 50% Pd coverage indicates that larger and higher palladium islands block some active sites of platinum either for methanol adsorption or for the adsorption and oxidation of reaction intermediates on Pd/Pt edges. Thus, a certain optimum coverage of palladium on platinum surface is necessary to produce the best electrocatalytic effect for methanol oxidation reaction.

The superior activity of 35% Pd/Pt(poly) for methanol oxidation with respect to both the negative shift of the onset potential and much higher peak current densities compared to both consisting metals indicates a strong synergistic effect. Similar effects are also observed for bimetallic surfaces with Pd as deposit for other reactions like formic acid oxidation on Pd/Pt [42], or ethanol oxidation on Pd/Au [45]. Several different explanations may be considered to interpret such effects taking into account possible different reaction pathways. A possible explanation might be that the reaction occurs through a bi-functional mechanism [46]. By this model, platinum and palladium atoms on the bimetallic Pd/Pt electrode surface play a specific role in the overall oxidation process (reaction 1), which proceeds through several elementary steps involving CO as an adsorbed poisoning intermediate [6,7,16]:

$$CH_3OH + 4OH^- \rightarrow CO_{ads} + 4H_2O + 4e^- \quad (5)$$

$$OH^- \rightarrow OH_{ads} + e^- \quad (6)$$

$$CO_{ads} + 2OH_{ads} + 2OH^- \rightarrow CO_3^{2-} + 2H_2O \quad (7)$$

This means that platinum atoms adsorb methanol dissociatively through reaction 5, while palladium atoms, being more oxophilic metal than platinum [33], adsorb OH radicals through reaction 6, at more negative potentials. This leads to an increase of the oxidation rate by increasing the rate of chemical surface reaction between methanol residue and OH^- radicals through an increase of OH^- concentration.

In order to get a better insight into possible reaction pathways responsible for such a superior activity of 35% Pd/Pt(poly) for methanol oxidation in comparison with bare Pd and Pt, the electrocatalytic activities of the same electrodes for CO and formaldehyde oxidation, as the most possible methanol oxidation reaction intermediates, are presented over the same potential range in Fig. 8. Methanol oxidation on 35% Pd/Pt(poly), Fig. 8a, occurs in a wider potential region compared to CO stripping (Fig. 8b), and peaks maxima for these two reactions do not coincide. Up to the potential of approx. −0.2 V, palladium is not active for CO oxidation, which leads to the assumption that at lower potentials methanol adsorption and its subsequent oxidation through carbonate pathway may take place only on platinum sites. It is worth noting that methanol oxidation and CO stripping on Pd(poly) occur at higher potentials, and over the same potential region. These considerations are in accordance with the assumption that at lower potential methanol oxidation on 35% Pd/Pt occurs through bifunctional or carbonate reaction pathway. Besides, the improved electrochemical response obtained for 35% Pd/Pt(poly) can be ascribed to the modification of the electronic properties by the interaction between the deposited Pd and the underlying Pt

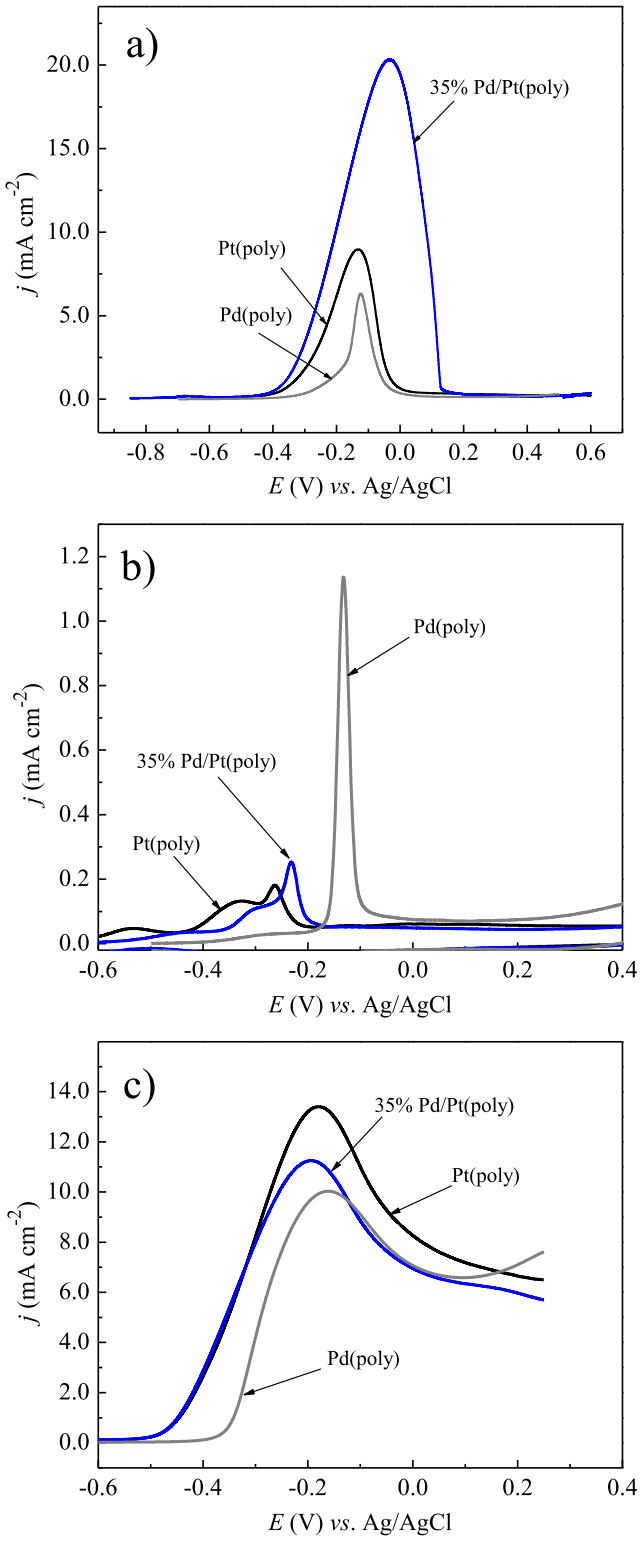

Fig. 8. Comparison of the electrocatalytic activity of 35% Pd/Pt(poly) with the activity of bare Pt and Pd for the oxidation of methanol, CO and formaldehyde. The anodic sweeps were taken from Figs. 5–7. Current densities are referred to the electrochemically active surface areas.

substrate. According to the literature [47–49], due to the electronic effect in which the d-band center of Pd is raised additionally by the presence of Pt, the adsorption of OH^- is promoted which facilitated the oxidation of adsorbed CO species. On the other hand, due to the presence of Pd, the position of the Pt d-band center can be changed which can cause the lowering of CO adsorption energy on Pt and thereby gives more free Pt active sites on the electrode surface.

In contrast to the activity of Pd modified Pt for CO oxidation, which falls in between the activities of consisting metals (see Fig. 5), their activity towards formaldehyde oxidation (see Fig. 6) shows a synergistic effect. Comparing methanol oxidation, Fig. 8a, and HCHO oxidation on 35% Pd/Pt and on bare Pt and Pd surfaces, Fig. 8c, it can be seen that these reactions occur over the same potential region. Namely, palladium atoms on platinum surface probably favor the methanol-reactive intermediate-formate path, which takes place at lower potentials [10] and inhibits the adsorption of CO intermediate [20,42]. Based on the previously exposed explanations, we can conclude that methanol oxidation on 35% Pd/Pt(poly) electrode occurs through parallel carbonate and formate pathways. Consequently, a remarkably high activity towards methanol oxidation was determined by the adsorption of OH species on Pd and Pd/Pt sites at lower potentials compared to their adsorption on Pt, which facilitates carbonate methanol oxidation pathway and by the ability of palladium islands to control the poisoning effects through the oxidation of formaldehyde as a reaction intermediate, which facilitates formate methanol oxidation pathway.

Additionaly, taking into account that at each surface investigated, CO is fully oxidized and that there is no CO adsorption at higher potentials, carbonate pathway for methanol oxidation is excluded, and the “direct pathway” of methanol electro-oxidation can be assumed [20,42]. A similar effect, in the case of formic acid electrooxidation on Pd/Pt nanoparticle catalyst in acidic medium, was obtained [42]. According to the activity of investigated surfaces for formaldehyde oxidation, it can also be assumed that, at higher potentials methanol oxidation occurs, at least partly through formate pathway.

Chronoamperometry curves, demonstrating the long–term activity of the most active 35% Pd/Pt(poly) electrode in comparison with the activity of bare Pt and Pd these electrodes are presented in Fig. 9. The curves were obtained by measuring the current density under a constant potential of −0.25 V for 30 min. A pronounced current decay in the first 2–3 min was found for all electrodes, which could derive from the accumulation of poisonous intermediates such as carbonaceous or CO species formed during methanol oxidation reaction [9]. With the test time elapsing,

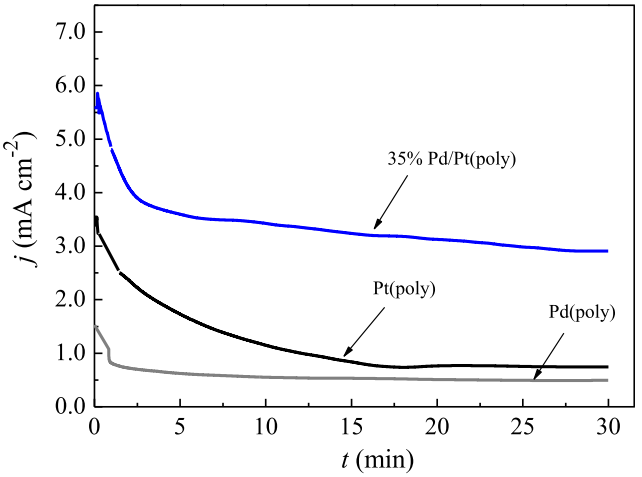

Fig. 9. Chronoamperometry measurements of the electrocatalytic activity of 35% Pd/Pt(poly), bare Pt and Pd for the oxidation of methanol in 0.1 M KOH. Curves are obtained by measuring current density under a constant potential of −0.25 V for 30 min. Current densities are referred to the electrochemically active surface areas.

current decay became much slower and finally reached the steady-state. The order of the activity in chronoamperometry tests was in good agreement with the order of activity in cyclic voltammetry measurements, confirming that 35% Pd/Pt(poly) electrode showed the highest activity for methanol oxidation reaction with the current density several times higher than that for bare Pt electrode.

The enhancement of the activity of 35% Pd/Pt(poly) surface with respect to the activity of bare Pt and bare Pd for methanol oxidation was compared with the enhancement of the activity of the other similar Pd/Pt systems including various carbon supported PdPt nanoparticles with respect to either bare Pt or Pt/C and Pd/C [50–54].

As shown above (Section 3.1.2.), generally much higher loading of Pd is needed for Pd/C systems, where the carbon substrate is not active for methanol oxidation, than in this case, where Pt(poly) as substrate is very active for methanol oxidation. Besides, at such low Pd loading as in this case of Pd/Pt catalyst, Pd/C catalyst would show no significant activity. Therefore, direct comparison of the activity with respect to Pd loadings, i.e. the comparison of the mass normalized currents is almost impossible. Instead, we made a comparison of the activity of our Pd/Pt(poly) electrodes with PdPt/C systems taking into account the relative content of both metals presented as a percentage of Pd and Pt in nanoparticles refs. [50–52].

In the case of PdPt/C electrodes, prepared by the electrochemical codeposition of Pt and Pd with the atomic ratio 1:2 [50], the relative enhancement of the methanol oxidation current with respect to Pt/C substrate is lower than the enhancement in the case of 35% Pd/Pt(poly) with respect to bare Pt. Besides, the current density maximum is achieved faster and at lower potential for methanol oxidation on 35% Pd/Pt(poly) than on PdPt/C, indicating faster reaction kinetics. In contrast to the hereby presented results, where the Pt:Pd ratio for the most active Pd/Pt(poly) surface was approximately 3:1, for PdPt nanoparticles supported on graphene, the one with Pt:Pd ratio of 1:3 exhibited the highest activity for methanol oxidation [51]. Pt–Pd nanoparticles with Pt; Pd ratio of 3:1, supported on reduced graphene oxide, have shown an excellent catalytic activity for methanol oxidation in alkaline media compared to commercial 10% Pd/C and 10% Pt/C [52]. Besides, the other Pd–Pt systems obtained by electrochemical deposition were also explored for the studies of methanol oxidation in alkaline media. [53,54]. Nanostructured Pd thin films electrochemically deposited on polycrystalline Pt, where the Pd content was in the range of 0.4 μg–0.8 μg, slightly higher than in our case, have shown an enhanced activity towards methanol oxidation with respect to bare Pt [53]. The maximum of the methanol oxidation current peak is about 3.5 times higher on Pd/Pt than on Pt electrode. Similarly enhanced activity for methanol oxidation in alkaline media was obtained for potentiostatically deposited Pd nanoparticles [54], which was ascribed to the significant increase of the electrochemically active surface area with respect to bare Pt substrate. In all mentioned cases, the onset potential for methanol oxidation is the same as on our 35% Pd/Pt(poly) bimetallic surface.

As shown in this work, roughly the Pd:Pt ratio of 1:2 has shown the best activity for methanol oxidation in alkaline media. This might be of crucial importance in the design of PtPd nanoparticles, particularly those highly dispersed on a nonmetallic substrate, with low Pt and Pd loadings, which might be obtained using spontaneous deposition method. This will be a matter of our future studies.

4. Conclusions

In this paper, we have demonstrated that the electrocatalytic activity of platinum towards methanol oxidation in alkaline solution could be significantly enhanced by the presence of spontaneously deposited Pd nanoislands. Simultaneously recorded height and phase AFM images of different Pd/Pt(poly) nanostructures enabled their proper characterization with respect to the lateral size, height and coverage of the deposited Pd islands. The additional information about the average Pd island heights was obtained using spectroscopic ellipsometry, while the oxidation state of the deposited Pd was revealed from XPS analysis.

Pt(poly) surface with 35% Pd coverage exhibited a superior catalysis for methanol oxidation reaction with respect to both consisting metals revealing a strong synergistic effect. The oxidation of CO and formaldehyde, as possible intermediates during methanol oxidation were also investigated in the same alkaline media in order to get a better insight into the origin of the synergistic effect. CO stripping peaks obtained for 25%, 35% and 50% Pd/Pt(poly) nanostructures shift positively with increasing Pd nanoislands coverage and fall in between potentials for CO oxidation on bare Pt(poly) and on bare Pd(poly). The electronic effect caused by the electronic interaction of Pd nanoislands and the underlying Pt substrate may lead to the lowering of binding energies of adsorbed reaction intermediates, such as CO_{ads} or OH_{ads} species, facilitating thus the carbonate methanol oxidation reaction pathway. On the other hand, the same 35% Pd/Pt(poly) surface is the most active for formaldehyde oxidation and exhibited similar synergistic effect as in the case of methanol oxidation indicating that the later one proceeds at least partly through formate pathway.

Acknowledgment

The work was supported by the Ministry of Science of Republic Serbia, project No 45005.

References

[1] A.S. Aricò, S. Srinivasan, V. Antonucci, Fuel Cells 1 (2001) 133–161.
[2] T. Iwasita, Electrochim. Acta 47 (2002) 3663–3674.
[3] B. Beden, F. Kardigan, C. Lamy, J.M. Leger, J. Electroanal. Chem. 127 (1981) 75–85.
[4] C.M. Johnston, S. Strbac, A. Lewera, E. Sibert, A. Wieckowski, Langmuir 22 (2006) 8229–8240.
[5] J.R. Varcoe, R.C.T. Slade, Electrochem. Commun. 8 (2006) 839–843.
[6] E. Hao Yu, K. Scott, R.W. Reeve, J. Electroanal.Chem. 547 (2003) 17–24.
[7] J.S. Spendelow, A. Wieckowski, Phys. Chem. Chem. Phys. 9 (2007) 2654–2675.
[8] M. Jing, L. Jiang, B. Yi, G. Sun, J. Electroanal. Chem. 688 (2013) 172–179.
[9] R. Manoharan, J. Prabhuram, J. Power Sources 96 (2001) 220–225.
[10] K. Matsuoka, Y. Iriyama, T. Abe, M. Matsuoka, Z. Ogumi, Electrochim. Acta 51 (2005) 1085–1090.
[11] T. Iwasita, in: Wolf Vielstich, Hubert A. Gasteiger, Arnold Lamm (Eds.), Methanol and CO electrooxidation, Handbook of Fuel Cells – Fundamentals, Technology and Applications, Electrocatalysis, Vol. 2, John Wiley & Sons, Ltd, 2003. ISBN: 0-471-49926-9.
[12] M. Koper, Surf. Sci. 548 (2004) 1–3.
[13] M. Krausa, W. Vielstich, J. Electroanal. Chem. 379 (1994) 307–314.
[14] T. Iwasita, H. Hoster, A. John-Anacker, W.F. Lin, W. Vielstich, Langmuir 16 (2000) 522–529.
[15] J.S. Spendelow, P.K. Babu, A. Wieckowski, Curr. Opin. Solid State Mater. Sci. 9 (2005) 37–48.
[16] A.V. Tripkovic, S. Strbac, K. Dj Popovic, Electrochem. Commun. 5 (2003) 484–490.
[17] Z. Liu, X.Y. Ling, X. Su, J.Y. Lee, J. Phys. Chem. B 108 (2004) 8234–8240.
[18] A. Santasalo-Aarnio, Y. Kwon, E. Ahlberg, K. Kontturi, T. Kallio, M. Koper, Electrochem. Commun. 13 (2011) 466–469.
[19] V. Stamenkovic, B.B. Blizanac, B.N. Grgur, N.M. Markovic, Chem. Ind. 56 (2002) 273–286.
[20] G. Gökagac, J.M. Leger, F. Hahn, Z. Naturforsch 58b (2003) 423–432.
[21] M. Smiljanic, Z. Rakocevic, A. Maksic, S. Strbac, Electrochim. Acta 117 (2014) 336–343.
[22] I. Horcas, R. Fernandez, J.M. Gomez-Rodriguez, J. Colchero, J. Gomez-Herrero, A.M. Baro, Rev. Sci. Instrum. 78 (2007) art. No. 013705.
[23] Horiba Scientific, DeltaPsi2 Software, Reference Manual, NP/DeltaPsi2R.Fm/264202–06/01/2010. Part Number: 31 087 091.
[24] F. Alcaide, G. Alvarez, P.L. Cabot, H.-J. Grande, O. Miguel, A. Querejeta, Int. J. Hydrog. Energy 36 (2011) 4433–4439.
[25] Z. Liu, X. Zhang, L. Hong, Electrochem. Commun. 11 (2009) 925–928.

[26] K.-H. Ye, S.-A. Zhou, X.-C. Zhu, C.-W. Xua, P.K. Shen, Electrochim. Acta 90 (2013) 108–111.
[27] L.K. Ono, B. Yuan, H. Heinrich, B. Roldan Cuenya, J. Phys. Chem. C. 114 (2010) 22119–22133.
[28] C.R. Parkinson, M. Walker, C.F. McConville, CAICISS LEED Surf. Sci. 545 (2003) 19–33.
[29] H. Gabasch, W. Unterberger, K. Hayek, B. Klotzer, E. Kleimenov, D. Teschner, S. Zafeiratos, M. Havecker, A. Knop-Gericke, R. Schlogl, J. Han, F.H. Ribeiro, B. Aszalos-Kiss, T. Curtin, D. Zemlyanov, Surf. Sci. 600 (2006) 2980–2989.
[30] T. Schalow, B. Brandt, M. Laurin, S. Schauermann, S. Guimond, H. Kuhlenbeck, J. Libuda, H.-J. Freund, Surf. Sci. 600 (2006) 2528–2542.
[31] G. Jerkiewicz, Electrocatal 1 (2010) 179–199.
[32] S. Strbac, Electrochim. Acta 56 (2011) 1597–1604.
[33] M. Arenz, V. Stamenkovic, P.N. Ross, N.M. Markovic, Surf. Sci. 573 (2004) 57–66.
[34] G. Jerkiewicz, in: A. Wieckowski (Ed.), Interfacial Electrochemistry: Experimental, Theory and Applications, Marcel Dekker, New York, 1999, pp. 559–576.
[35] S.J. Xia, V.I. Birss, Electrochim. Acta 45 (2000) 3659–3673.
[36] C.-C. Hu, T.-C. Wen, Electrochim. Acta 40 (1995) 495–503.
[37] M. Grden, M. Lukaszewski, G. Jerkiewicz, A. Czerwinski, Electrochim. Acta 53 (2008) 7583–7598.
[38] G. Macfie, A. Cooper, M.F. Cardosi, Electrochim. Acta 56 (2011) 8394–8402.
[39] J.S. Spendelow, G.Q. Lu, P.J.A. Kenis, A. Wieckowski, J. Electroanal. Chem. 568 (2004) 215–224.
[40] M.C. Perez, A. Rincon, C. Gutierrez, J. Electroanal. Chem. 511 (2001) 39–45.
[41] N.M. Markovic, T.J. Schmidt, B.N. Grgur, H.A. Gasteiger, R.J. Behm, P.N. Ross, J. Phys. Chem. B 103 (1999) 8568–8577.
[42] P. Waszczuk, T.M. Barnard, C. Rice, R.I. Masel, A. Wieckowski, Electrochem. Commun. 4 (2002) 599–603.
[43] K. Nishimura, K. Kunimatsu, M. Enyo, J. Electroanal. Chem. 260 (1989) 167–179.
[44] A.C. Garcia, V.A. Paganin, E.A. Ticianelli, Electrochim. Acta 53 (2008) 4309–4315.
[45] C.-H. Cui, J.-W. Yu, H.-H. Li, M.-R. Gao, H.-W. Liang, S.-H. Yu, ACS Nano 5 (2011) 4211–4218.
[46] M. Watanabe, S. Motoo, J. Electroanal. Chem. 60 (1975) 267–273.
[47] E. Christoffersen, P. Liu, A. Ruban, H.L. Skriver, J.K. Nørskov, J. Catal. 199 (2001) 123–131.
[48] L.C. Grabow, B. Hvolbæk, J.K. Nørskov, Top. Catal. 53 (2010) 298–310.
[49] B. Hammer, J.K. Norskov, Adv. Catal. 45 (2000) 71–129.
[50] S.S. Mahapatra, A. Dutta, J. Datta, Int. J. Hydrog. Energy 36 (2011) 14873–14883.
[51] Y. Zhang, G. Chang, H. Shu, M. Oyama, X. Liu, Y. He, J. Power Sources 262 (2014) 279–285.
[52] S.-S. Li, J.-J. Lv, Y.-Y. Hu, J.-N. Zheng, J.-R. Chen, A.-J. Wang, J.-J. Feng, J. Power Sources 247 (2014) 213–218.
[53] J. Zhang, M. Huang, Houyi Ma, F. Tian, W. Pan, S. Chen, Electrochem. Commun. 9 (2007) 1298–1304.
[54] R. Gupta, S.K. Guin, S.K. Aggarwal, Electrochim. Acta 116 (2014) 314–320.